UDC 621.313 https://doi.org/10.20998/2074-272X.2022.1.01

M.M. Zablodskiy, V.E. Pliuhin, S.I. Kovalchuk, V.O. Tietieriev

Indirect field-oriented control of twin-screw electromechanical hydrolyzer

Goal. *Development of a mathematical model of indirect field-oriented control of a twin-screw electromechanical hydrolyzer.* ***Methodology****. The paper presents a mathematical model of Indirect field-oriented control of twin-screw electromechanical hydrolyzer. The mathematical model was developed in the MATLAB / Simulink software environment. The determination of the main parameters of a twin-screw electromechanical hydrolyzer was carried out by developing a finite element model in the Comsol Multiphysics software environment.* ***Results****. Based on the results of a mathematical study, graphical dependences of the distribution of magnetic induction in the air gap of a ferromagnetic rotor, a spatial representation of the distribution of magnetic induction on a 3D model of a ferromagnetic rotor of a twin-screw electromechanical hydrolyzer were obtained. The results of finite element modeling were confirmed by a practical study of a mock-up of a ferromagnetic rotor of a twin-screw electromechanical hydrolyzer. By implementing the MATLAB / Simulink model, graphical dependences of the parameters of the ferromagnetic rotor of a twin-screw electromechanical hydrolyzer are obtained under the condition of a stepwise change in the torque and a cyclic change in the angular velocity.* ***Originality****. The paper presents an implementation of the method of indirect field-oriented control for controlling the ferromagnetic rotor of a twin-screw electromechanical hydrolyzer. The work takes into account the complex design of the ferromagnetic rotor of a twin-screw electromechanical hydrolyzer.* ***Practical significance.*** *The practical implementation of the results of mathematical modeling makes it possible to achieve effective control of a complex electromechanical system, allows further research to maintain the necessary parameters of the technological process and to develop more complex intelligent control systems in the future.* References 19, tables 4, figures 21.
Key words: **Maxwell's equations, field-oriented control, polyfunctional electromechanical converters, hydrolyzer, dissipative energy.**

У статті детально розглянуто конструктивні і електромагнітні особливості нестандартного електромеханічного перетворювача енергії – двошнекового електромеханічного гідролізера. Це технічний пристрій з поліфункціональними властивостями, здатний одночасно нагрівати, диспергувати, транспортувати, перемішувати та піддавати впливу магнітним полем в одному пристрої робочу сировину. Розроблено коло-польові та математичні моделі електромагнітних перехідних процесів цього пристрою. Основні параметри електромеханічної системи визначено шляхом кінцево-елементного моделювання та практичного дослідження феромагнітного ротора. В роботі представлено керування обертовим моментом та кутовою швидкістю феромагнітного ротора двошнекового електромеханічного гідролізера шляхом непрямого полеорієнтованого керування. Шляхом реалізації MATLAB / Simulink моделі отримано графічні залежності основних параметрів феромагнітного ротора за умов ступінчатої зміни обертового моменту та циклічної зміни кутової швидкості. За результатами моделювання помітно доцільність застосування методу непрямого керування з орієнтацією на поле для ефективного керування технологічним процесом двошнекового електромеханічного гідролізера. В порівнянні з розглянутими методами керування, непряме керування з орієнтацією на поле більш просте в проектуванні та реалізації, дозволяє досягнути бажаних характеристик та відкриває подальші можливості для дослідження двошнекового електромеханічного гідролізера. Бібл. 19, табл. 4, рис. 21.
Ключові слова: **рівняння Максвелла, непряме керування з орієнтацією на поле, поліфункціональний електромеханічний перетворювач, гідролізер, дисипативна енергія.**

Introduction. Efficient use of energy resources is an important task for today. The development of energy-saving technologies is directly related to increasing the efficiency of individual elements of the system, integrating the functional features of the system in one device and the use of dissipative energy. Since the increase in efficiency, provided that a certain level of system optimization is achieved, is achieved by developing new active and insulating materials, the methods of increasing it are limited. For technological systems that combine the processes of movement, heating and mixing of materials, the method of using dissipative energy should be considered the most effective [1]. Under the conditions of the previously mentioned integration of functional features of the system in one device and the use of dissipative energy, it becomes possible to save resources that under traditional schemes of energy conversion and use were spent, dissipated as heat into the environment.

Within the method of dissipative energy use, a double-screw electromechanical hydrolyzer has been developed for the processing of poultry by-products under the influence of a magnetic field. A double-screw electro-mechanical hydrolyzer is a technical device with poly-functional properties, capable of simultaneously heating, dispersing, transporting, mixing and exposing to a magnetic field in one device. The main working element of the double-screw electromechanical hydrolyzer is a ferromagnetic rotor (Fig. 1). The ferromagnetic rotor simultaneously acts as the rotor of the induction motor, heater, working element and protective shell [2].

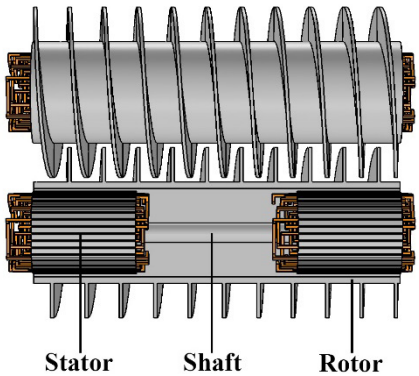

Fig. 1. Ferromagnetic double-screw rotor electromechanical hydrolyzer

The electromagnetic system of a double-screw electromechanical hydrolyzer consists of stators rigidly mounted on a fixed shaft. During the flux of current through the stator windings, they create electromagnetic moments that drive the ferromagnetic rotor.

Since the double-screw electromechanical hydrolyzer is a device that combines several technological processes, it is necessary to ensure effective control of the electromagnetic torque and rotation speed of the ferromagnetic rotor. Obtaining the necessary parameters of speed and torque is possible under the control of the joint operation of two stators, one of which operates in motor mode, the other – in generator mode, but with increasing stiffness of the resulting characteristics significantly reduces the overload capacity of the unit, developing another more effective management method.

Analysis of recent research and publications. Methods of controlling electric machines of alternating current are a difficult task. In the field of highly effective methods of speed and torque control, two methods have become the most widespread – field-oriented control and direct torque control [3-5]. In most cases, these methods are sufficient to meet most industrial needs, but due to the rapid development of digital technologies, more and more research is being conducted in the field of nonlinear control [6]. Recent publications include many works on various methods of controlling electric machines. The control of an induction motor by the method of indirect field-oriented control, considering the influence of perturbations of the rotor resistance, was performed in [3, 7]. The general recommendations for the design of the control system are given in the works, the criteria of stability and the minimum necessary phase conditions for the torque control are indicated, the results of the experimental study of a typical induction motor are presented. In [8], a method of predicted current control with field orientation was described, which was developed for a three-level inverter with a fixed neutral point for controlling a three-phase induction motor. The algorithm for calculating the optimal switching vector was used in the method, the control circuit of the stator voltage, stator current and motor's rotor speed was determined. The simulation results have a slight error when calculating the rotor flux and stator current. Sensorless direct torque control of an induction motor powered by a seven-level inverter using neural networks and fuzzy logic controller is presented in [9], fuzzy PI controller is used to control rotor speed, and artificial neural network is used to stator voltage. The method proposed in this work allows to control the torque, reduce the harmonic distortion of the stator current, improve the dynamic characteristics and reliability of the system. The method of operating cycle control, which is chosen to reduce the pulsation of torque and magnetic flux with direct torque control, is presented in [10]. A new algorithm for accurate selection of active voltage has been developed, the optimal duration of switching on at simultaneous control of stator magnetic flux and electric torque has been determined. According to the results of the study, the presented method provides less pulsations of torque and magnetic flux compared to the traditional method of direct torque control and a model that provides a better model of predicted current control. In [11], a model of predicted torque and magnetic flux based on perturbations was developed; the method of perturbation suppression is improved to ensure compatibility with the theory of finite sets; perturbation is provided for all possible switching states. According to the research results, this method improves the stability of the response of torque and current, significantly increases the resistance of the system *to changes in the values of the stator and rotor resistance* in comparison with traditional control methods.

The methods presented in [7-11], built on the basis of complex algorithms of neural networks and fuzzy logic, allow to effectively control the parameters of electric machines, however, at the same time, they have certain disadvantages: high complexity of algorithms, a large number of controlled parameters, high design load and the need for a full-fledged system model [12, 13].

The double-screw electromechanical hydrolyzer is a new electric machine and most of its parameters and characteristics still need detailed research. From the existing research, a complete picture of the magnetic field of the ferromagnetic rotor of a double-screw electromechanical hydrolyzer is known [2, 14]. This allows to conclude that for its management it is advisable to use the method of field-oriented control.

The aim of the work is to study the electromagnetic processes in a ferromagnetic rotor of a double-screw electromechanical hydrolyzer and to evaluate the feasibility of using the hydrolyzer indirect field-oriented control method.

Presenting main material. Due to its simplicity, indirect field-oriented control is one of the most effective ways to control an AC machine. For effective control of torque and speed, the stator current components in the model must be separated from the vector magnetic flux of the rotor [15]. Since it is necessary to know the parameters of an electric machine to develop a model of indirect control with field orientation, there is a need to develop a mathematical model of the ferromagnetic rotor of a double-screw electromechanical hydrolyzer, where it is not needed to know these parameters.

Finite element model in the time domain of the study. Due to the need for high accuracy, as well as due to the peculiarities of the design and the need to reduce the time for design, we used the software environment Comsol Multiphysics. The analysis of the electromagnetic field is performed based on the system of Maxwell's equations.

The magnetization of the ferromagnetic rotor is given as the *B-H* curve and is determined from the equation:

$$B = f\left(|H|\right)\frac{H}{|H|}. \qquad (1)$$

Multi-turn stator windings are used as a current source in the model (Fig. 2).

In the diagram (Fig. 2) the beginning of the corresponding phases (conductors leave the groove) is marked in capital letters (*A, B, C*) and the end (conductors enter the slot) in small letters (*a, b, c*).

The current density in the winding, A/m^2:

$$J_e = \frac{N \cdot I_{coil}}{A} \cdot e_{coil}, \qquad (2)$$

where N – winding turns; A – winding cross-section, m^2; I_{coil} – current in stator coil, A; e_{coil} – vector variable (to visualize the direction of winding turns).

The simulation was performed for a ferromagnetic rotor, the finite element mesh of the model (Fig. 3) was created in the software environment Comsol Multiphysics. Particular attention was paid to the air gap

at the interface between the stator and rotor of the electromechanical device. Statistics on the parameters of the mesh are given in Table. 1.

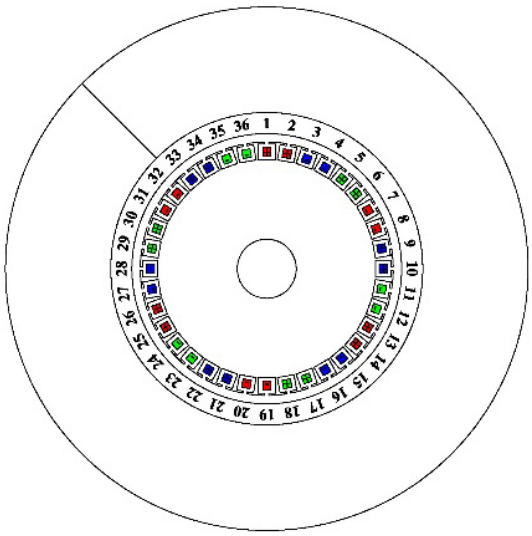

Fig. 2. Stator winding circuit

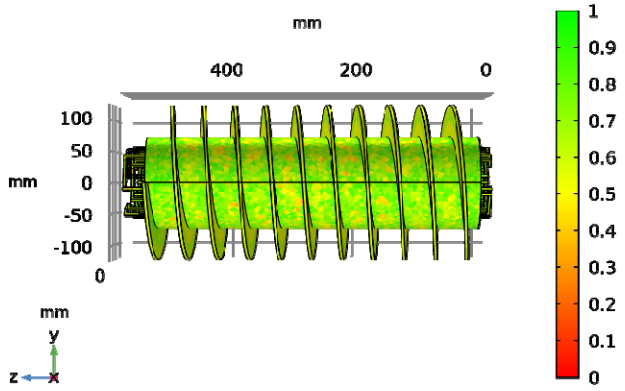

Fig. 3. Finite element mesh for ferromagnetic rotor model of double-screw electromagnetic hydrolyzer

Table 1

Parameters of the model finite element mesh

Mesh parameters	Values
Number of mesh vertices	241325
Tetrahedra	1444151
Triangles	277074
Edge elements	49887
Vertex elements	2759
Number of elements	1444151
Minimum element quality	0,0307
Average element quality	0,613
Element volume ratio	2,027E-6
Mesh volume	1,251E8 mm^3

MATLAB / Simulink model of indirect control with field orientation. In the case of low-speed orientation and for position control using an integration sensor-based flux sensor, a field-oriented indirect control model may not be acceptable for complex electromechanical systems. An alternative may be indirect control with field orientation without measuring the flux in the air gap [16]. Under such conditions, the torque can be regulated by the q-component of the stator current i_{qs}^{e} and the difference in the angular frequencies of the magnetic field of the stator and rotor $\omega_e - \omega_e$. The rotor flux can be regulated by the d-component of the stator current i_{ds}^{e}. Setting some desired value of the magnetic flux of the rotor $\lambda_r^{'*}$, the desirable d- component of the stator current i_{ds}^{e*} can be obtained from the equation:

$$\lambda_{dr}^{'*} = \frac{r_r^{'} L_m}{r_r^{'} + L_r^{'} p} i_{ds}^{e*}, \tag{3}$$

where $\lambda_{dr}^{'*}$ – desirable d-component of the rotor current, Wb; $r_r^{'}$ – induced active resistance of the rotor winding, Ω; L_m – mutual induction of stator windings, T; p – number of pole pairs.

For the desired torque value T_{em}^{*} at a certain value of the rotor flux, the desired value q-components of the stator current i_{qs}^{e} described by the equation:

$$T_{em}^{*} = \frac{3}{2} \cdot \frac{P}{2} \cdot \frac{L_m}{L_r^{'}} \lambda_{dr}^{'e*} i_{qs}^{e*}, \tag{4}$$

where P – power, W; $L_r^{'}$ – transient inductance of the rotor, H.

Because at a certain orientation of the field $i_{dr}^{'e}$ equal to zero and $\lambda_{dr}^{'e} = L_m i_{ds}^{e}$, then the desired angular speed of the rotor ω_2^{*} (rad/s) described by the equation:

$$\omega_2^{*} = \omega_e - \omega_r = \frac{r_r^{'} i_{qs}^{e*}}{L_r^{'} i_{ds}^{e*}}, \tag{5}$$

where ω_e – angular rotation velocity of the magnetic field, rad/s; ω_r – angular rotation speed of the rotor, rad/s.

The measured flux in the air gap is the resultant or reciprocal flux. This is not the same as the current connecting the rotor winding, whose angle ρ is the desired angle for field orientation. But, as the following equations shows, in combination with the measured stator current, it is possible to determine the value of ρ and the magnitude of the rotor flux. The measured stator currents abc are first converted to a stationary current qd using the equations:

$$i_{qs}^{s} = \frac{2}{3} i_{as} - \frac{1}{3} i_{bs} - \frac{1}{3} i_{cs}, \tag{6}$$

$$i_{ds}^{s} = \frac{1}{\sqrt{3}} \left(i_{cs} - i_{bs} \right). \tag{7}$$

The flux coupling of the rotor on the q axis in a fixed coordinate system can be expressed as:

$$\lambda_{qr}^{'s} = \left(L_m + L_{lr}^{'} - L_{lr}^{'} \right) \cdot i_{qs}^{s} + \left(L_m + L_{lr}^{'} \right) \cdot i_{qr}^{'s}. \tag{8}$$

Because λ_{mq}^{s} equal to $L_m \left(i_{qs}^{s} + i_{qr}^{'s} \right)$, it is possible to define $\lambda_{qr}^{'s}$ by measured values, i.e.

$$\lambda_{qr}^{'s} = \frac{L_r^{'}}{L_m} \lambda_{mq}^{s} - L_{lr}^{'} i_{qs}^{s}. \tag{9}$$

Similarly, $\lambda_{dr}^{'s}$ can be determined from

$$\lambda'^{s}_{dr} = \frac{L'_r}{L_m}\lambda^{s}_{md} - L'_{lr} i^{s}_{ds}. \quad (10)$$

Using calculated λ'^{s}_{qr} and λ'^{s}_{dr}, lets determine the cosine and sine ρ by geometric ratios:

$$\sin\left(\frac{\pi}{2}-\rho\right) = \cos\rho = \frac{\lambda'^{s}_{dr}}{\left|\lambda'^{s}_{r}\right|}, \quad (11)$$

$$\cos\left(\frac{\pi}{2}-\rho\right) = \sin\rho = \frac{\lambda'^{s}_{qr}}{\left|\lambda'^{s}_{r}\right|}, \quad (12)$$

where

$$\left|\lambda'^{e}_{r}\right| = \left|\lambda'^{s}_{r}\right| = \sqrt{\lambda'^{s2}_{dr} + \lambda'^{s2}_{qr}}. \quad (13)$$

The above calculations (6) – (13) are performed inside the field orientation unit. Estimated value $\left|\lambda'^{e}_{r}\right|$ returns to the inlet of the flux regulator that control the flux in the air gap. Values are calculated inside the torque calculation unit λ'^{e}_{r} and i^{e}_{qs} are used to estimate the value of the torque produced by the machine, then the calculated torque is returned to the input of the torque regulator.

The corresponding output data of the torque and flux regulators are the values of the commands, i^{e*}_{qs} and i^{e*}_{ds}, in the field-oriented rotor frame of reference. The transformations from *qde* to *qds* and *qds* to balanced *abc* take place in the whole unit of the *qd* to *abc* conversion unit:

$$\begin{cases} i^{s*}_{qs} = i^{e*}_{qs}\cos\rho + i^{e*}_{ds}\sin\rho; \\ i^{s*}_{ds} = -i^{e*}_{qs}\sin\rho + i^{e*}_{ds}\cos\rho; \\ i^{*}_{as} = i^{s*}_{qs}; \\ i^{*}_{bs} = -\frac{1}{2}i^{s*}_{qs} - \frac{\sqrt{3}}{2}i^{s*}_{ds}; \\ i^{*}_{cs} = -\frac{1}{2}i^{s*}_{qs} + \frac{\sqrt{3}}{2}i^{s*}_{ds}. \end{cases} \quad (14)$$

The orientation of the stator current field can also be achieved by applying the appropriate stator voltages. Since the strategy in the field-oriented circuit is to avoid disrupting the rotor flux connection as much as possible in response to changes in load torque, we can use a transient model in combination with properly oriented stator currents *qd* to determine stator voltage. Field-oriented stator currents *qd* are determined by converting the measured *abc* currents to stationary *qd* and values ρ in the following transformation

$$i^{e}_{qs} = i^{s}_{qs}\cos\rho - i^{s}_{ds}\sin\rho; \quad (15)$$

$$i^{e}_{ds} = i^{s}_{qs}\sin\rho + i^{s}_{ds}\cos\rho. \quad (16)$$

In the transient model for a situation where it can be assumed that the flux coupling of the rotor remains constant, the machine can be represented by a constant voltage on the transient inductance of the stator.

Stator flux coupling can only be expressed through stator currents and rotor flux coupling, i.e.

$$\lambda^{e}_{qs} = L'_s i^{e}_{qs} + \frac{L_m}{L'_r}\lambda'^{e}_{qr}; \quad (17)$$

$$\lambda^{e}_{ds} = L'_s i^{e}_{ds} + \frac{L_m}{L'_r}\lambda'^{e}_{dr}; \quad (18)$$

$$L'_s\frac{di^{e}_{qs}}{dt} + \frac{L_m}{L'_r}\frac{d\lambda'^{e}_{qr}}{dt} = v^{e}_{qs} - r_s i^{e}_{qs} - E'_{qs} - \omega_e L'_s i^{e}_{ds}; \quad (19)$$

$$L'_s\frac{di^{e}_{ds}}{dt} + \frac{L_m}{L'_r}\frac{d\lambda'^{e}_{dr}}{dt} = v^{e}_{ds} - r_s i^{e}_{ds} - E'_{ds} + \omega_e L'_s i^{e}_{qs}. \quad (20)$$

Setting the derivatives of the time of flux coupling of the rotor to zero and rearranging so that the left side contains the sum of the voltage across the transient resistance and the voltage drop across the transient resistance of the stator, then we obtain

$$r_s i^{e}_{qs} + L'_s\frac{di^{e}_{qs}}{dt} + E'_{qs} = v^{e}_{qs} - \omega_e L'_s i^{e}_{ds}; \quad (21)$$

$$r_s i^{e}_{ds} + L'_s\frac{di^{e}_{ds}}{dt} + E'_{ds} = v^{e}_{ds} + \omega_e L'_s i^{e}_{qs}. \quad (22)$$

By adjusting the outputs of the torque and flux controllers for the cross-current, we obtain the required command values for v^{e}_{qs} and v^{e}_{ds}. The command values for the stator voltages *abc* can be calculated as follows

$$\begin{cases} v^{s*}_{qs} = v^{e}_{qs}\cos\rho + v^{e}_{ds}\sin\rho; \\ v^{s*}_{ds} = -v^{e}_{qs}\sin\rho + v^{e}_{ds}\cos\rho; \\ v^{*}_{as} = v^{s*}_{qs}; \\ v^{*}_{bs} = -\frac{1}{2}v^{s*}_{qs} - \frac{\sqrt{3}}{2}v^{s*}_{ds}; \\ v^{*}_{cs} = -\frac{1}{2}v^{S*}_{qs} + \frac{\sqrt{3}}{2}v^{s*}_{ds}. \end{cases} \quad (23)$$

The desired rotor speed less than the nominal with a certain nominal supply voltage is described by equations:

$$\left(v^{e}_{qs} - jv^{e}_{ds}\right) = \left(r_s + j\omega_e L'_s\right)\cdot\left(i^{e}_{qs} - ji^{e}_{ds}\right) + \left(E'_{qs} - jE'_{ds}\right); \quad (24)$$

$$T'_0 = \frac{x'_{lr} + x_m}{\omega_e r'_r}, \quad (25)$$

where v^{e}_{qs}, v^{e}_{ds} – q and d voltage components, V; r_s – stator winding resistance, Ω; L'_s – stator inductance, H; E'_{qs}, E'_{ds} – q and d component of the magnetizing voltage, V; x'_{lr} – inductive scattering resistance of the rotor winding, Ω; x_m – inductive resistance of the stator core magnetization, Ω.

Simulation results. Finite element modeling was performed for the model with the parameters given in Table. 2.

The materials of the model were chosen:

- *Soft Iron* (without losses) – as a material of stator core;
- *Iron* – as the shaft material;
- *Copper* – as the stator winding material.

Table 2

Parameters of the stator double-screw electromechanical hydrolyzer

Selected materials	
Current in stator winding	10,5 A
Simulation time	Range (0, 0.1, 1) s

Materials were selected from the library of materials of the Comsol software environment. As a material for the ferromagnetic rotor was chosen steel grade St3, the magnetization curve of which is shown in Fig. 4.

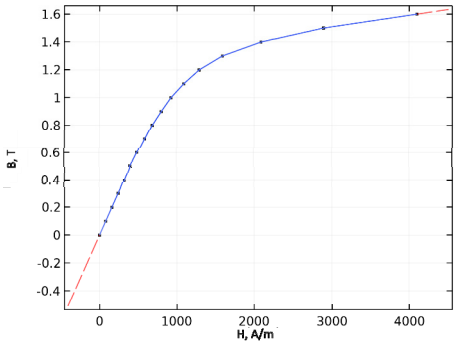

Fig. 4. B-H steel St3 magnetization curve

The picture of the distribution of magnetic induction for the nominal mode of operation of the ferromagnetic rotor of a double-screw electromechanical hydrolyzer is presented in Fig. 5.

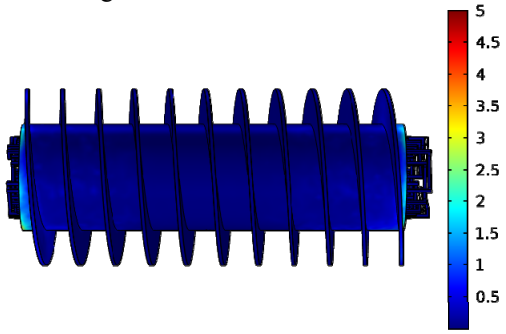

Fig. 5. Magnetic induction distribution pattern for the model ferromagnetic rotor of a double-screw electromechanical hydrolyzer, T

Graphical representation of the distribution of magnetic induction in the air gap of the ferromagnetic rotor of a double-screw electromechanical hydrolyzer, at the beginning and end of the simulation is presented in Fig. 6.

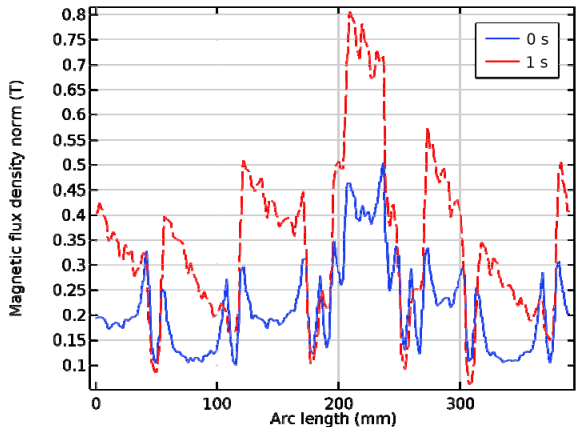

Fig. 6. Graphical representation of the distribution of magnetic induction in the air gap of a double-screw electromechanical hydrolyzer

For quantitative assessment in Table 3 shows the average and maximum values of magnetic flux density in the air gap of a double-screw electromechanical hydrolyzer.

Table 3

Average and maximum values of magnetic flux density in the air gap of the double-screw electromechanical hydrolyzer

Time, s	Average value, T	Maximum value, T
0	0,216174	0,46575
0,1	0,347887	0,794864
0,2	0,348252	0,796307
0,3	0,348275	0,796473
0,4	0,348284	0,796515
0,5	0,348277	0,796508
0,6	0,348277	0,796515
0,7	0,348278	0,79652
0,8	0,348277	0,79652
0,9	0,348285	0,796534
1	0,348285	0,796536

According to the simulation results, it is noticeable that the discrete arrangement of the stators along the axial line of the ferromagnetic rotor of the double-screw electromechanical hydrolyzer forms stable zones with a cyclic level of magnetic field intensity. Around the air gap of the double-screw electromechanical hydrolyzer 6 narrow and wide zones, alternating with each other [14].

The main results of modulation were compared with the data obtained from the experimental study of the auger of the electromechanical hydrolyzer (Fig. 7).

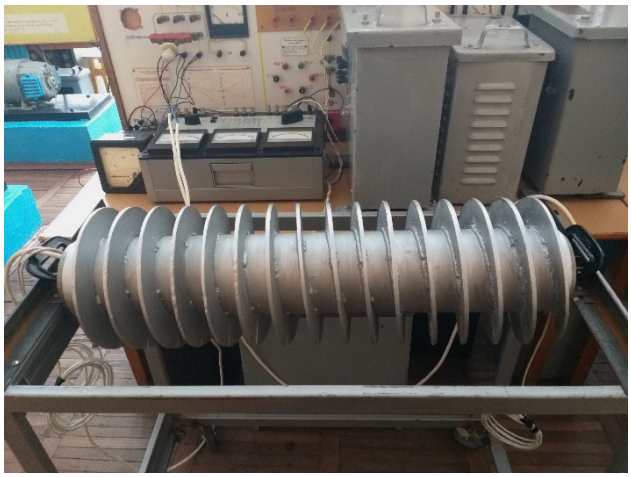

Fig. 7. Experimental sample of an electromechanical hydrolyzer

During the research, magnetic induction was measured using MagneticFeldMeterTM-191 and PCE-MFM 4000 instruments (Fig. 8).

The average values of deviations between the results of mathematical and experimental research are 0.13 T, which is 2-3% in the measurement range of 0.4–0.8 T, so the mathematical model can be considered correct and used in further research.

Fig. 8. Measuring instruments MagneticFeldMeterTM-191 and PCE-MFM 4000

MATLAB / Simulink model of indirect control with field orientation is made for one stator of a double-screw electromechanical hydrolyzer with the parameters specified in Table 4. From studies of the electromechanical characteristics of the double-screw electromechanical hydrolyzer [14] it is known that the nominal speed of the working body (ferromagnetic rotor) is 200 rpm. Since it is known that the stator contains 6 poles, the slip calculated as following:

$$s = \frac{(n_1 - n_2)}{n_1} = \frac{(1000 - 200)}{1000} = 0.8$$

where n_1 – synchronous speed, rpm; n_2 – actual speed, rpm.

Table 4

Parameters of the replacement scheme for one stator and a ferromagnetic rotor of a double-screw electromechanical hydrolyzer

Parameter	Value
Power	1400 W
Rated voltage	118 V
Rated current	10,5 A
Power factor	0,65
Number of pole pairs	6
Rated frequency	50 Hz
Rated slip	0,8
Rated rotation speed	1000 rpm
Stator winding resistance	200 rpm
Reactive scattering resistance stator windings	0,1323 Ω
Reactive scattering resistance rotor windings	0,2033 Ω
Reactive magnetization resistance stator windings	0,2372 Ω
Rotor winding resistance	5,0475 Ω
The inertia of the rotor	0,174 Ω

The scheme of replacement of the double-screw electromechanical hydrolyzer is presented in Fig. 9-11.

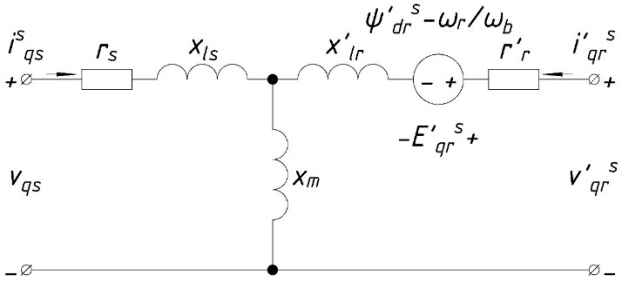

Fig. 9. Scheme of stator replacement of ferromagnetic rotor of double-screw electromechanical hydrolyzer in reference system q-axis

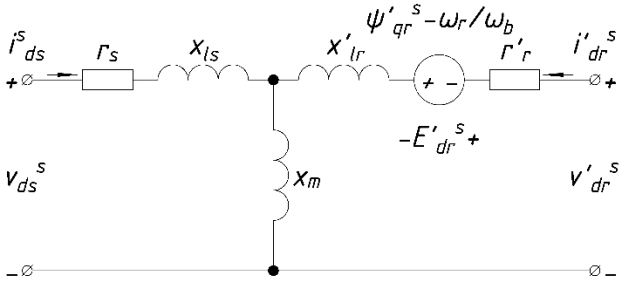

Fig. 10. Scheme of replacement of a stator of a ferromagnetic rotor of a double-screw electromechanical hydrolyzer in the frame of reference d-axis

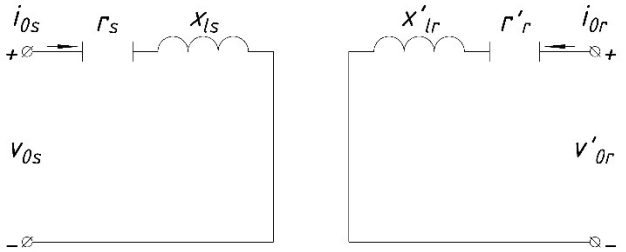

Fig. 11. Scheme of stator replacement of ferromagnetic rotor of double-screw electromechanical hydrolyzer in reference system zero-sequence

In Fig. 12 a general Simulink model of indirect control with field orientation is shown. To reduce the duration of the model calculation, the work does not consider the transients that occur in the PWM converter during control, only the main components of the output voltages are taken into account [18, 19].

Figure 13 presents the implementation of the non-direct control unit with field orientation. Values are calculated in the middle of the block i_{ds}^{e*}, i_{qs}^{e*}, ω_2^*, angle θ – the sum of the rotor rotation angle θ_2 and the angle of sliding integrated from the rotor rotation sensor θ_r. In the middle of the block *qde2abc* (Fig. 12) is the generation of reference *abc* currents.

During the simulation, two types of control were implemented. The first one is a step change of the torque according to the desired, fixed value of the angular velocity of rotation (Fig. 14 – Fig. 17).

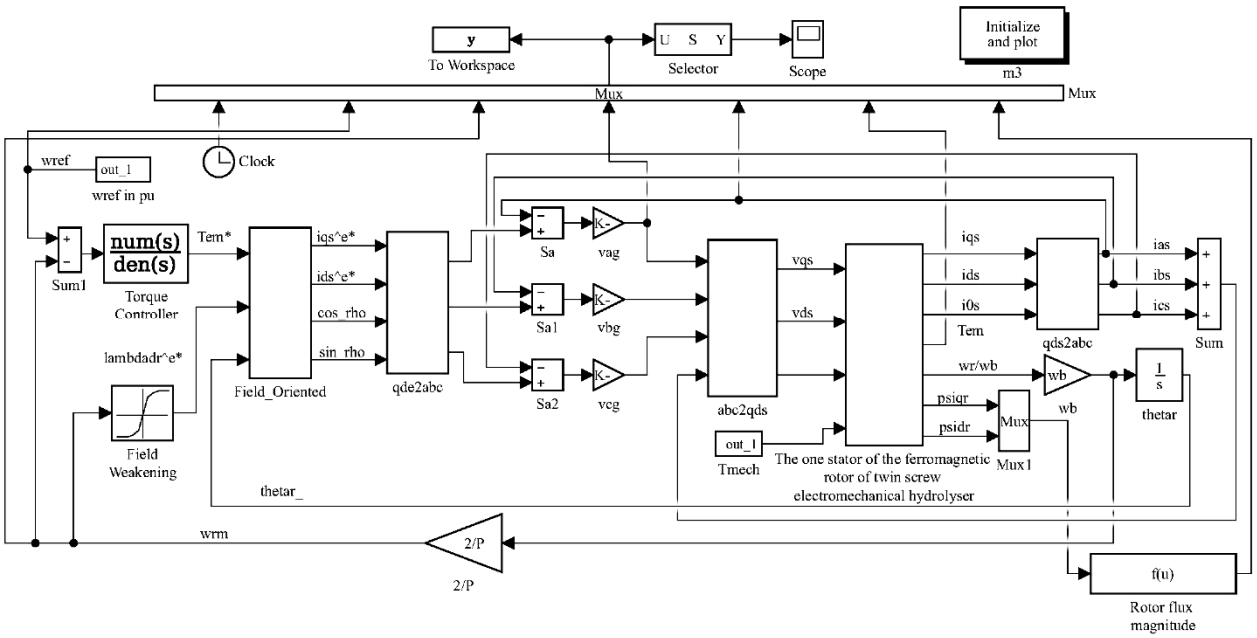

Fig. 12. MATLAB / Simulink model of double-screw electromechanical hydrolyzer with indirect control with field orientation

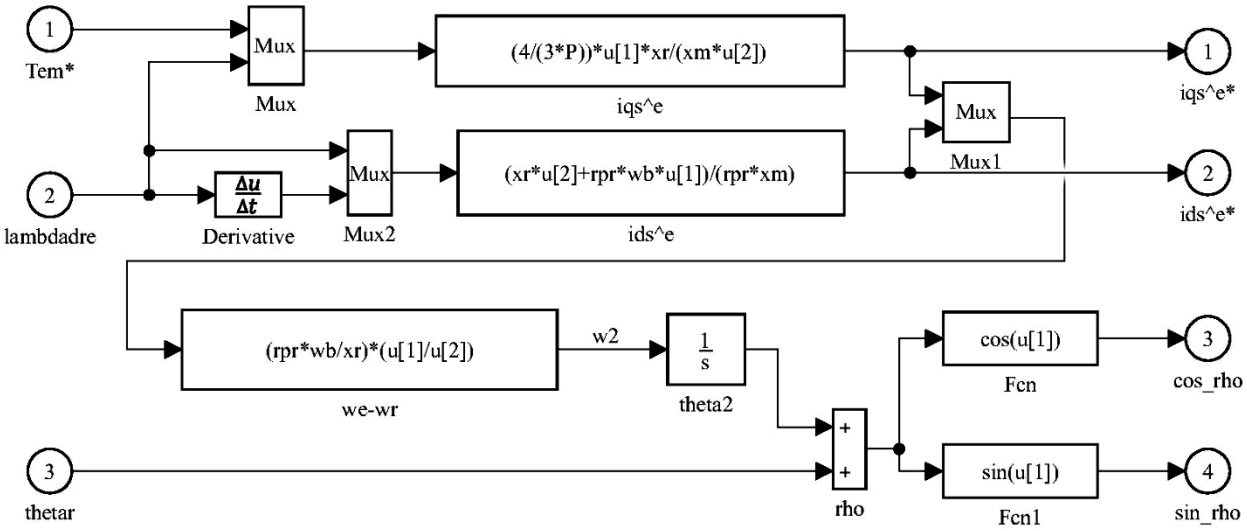

Fig. 13. Implementation of the model of indirect control of two-screw electromechanical hydrolyzer with field orientation

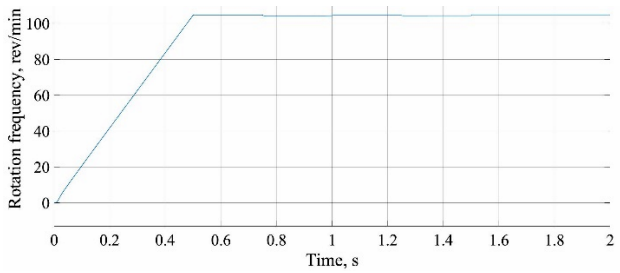

Fig. 14. Angular speed during start-up and loading, rad / s

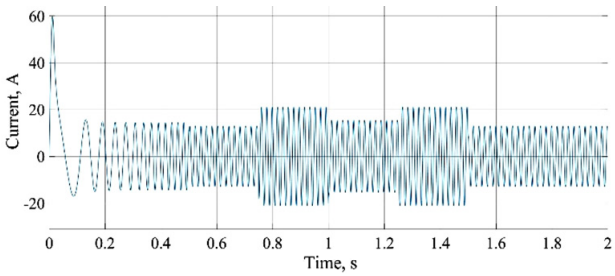

Fig. 16. Current during start-up and loading, A

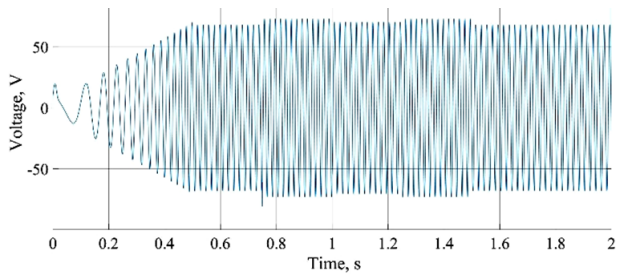

Fig. 15. Voltage during start-up and loading, V

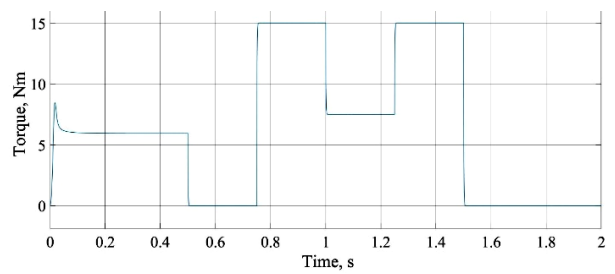

Fig. 17. Torque during start-up and loading, Nm

The second one is a cyclic change in the angular rotation velocity (Fig. 18 – Fig. 21).

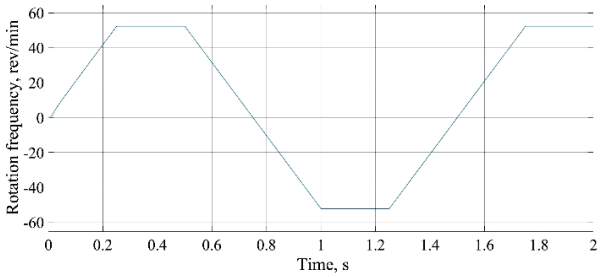

Fig. 18. Change of angular velocity during idle mode, rad / s

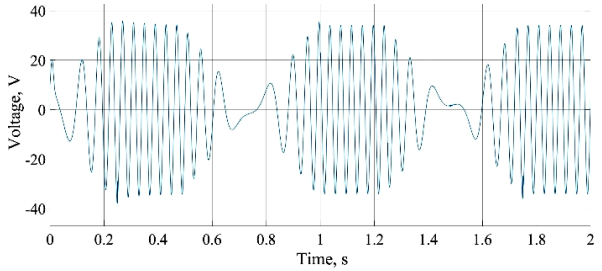

Fig. 19. Voltage dependents in idle mode, V

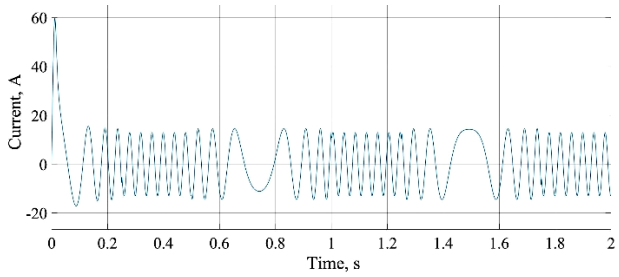

Fig. 20. Current dependents in idle mode, A

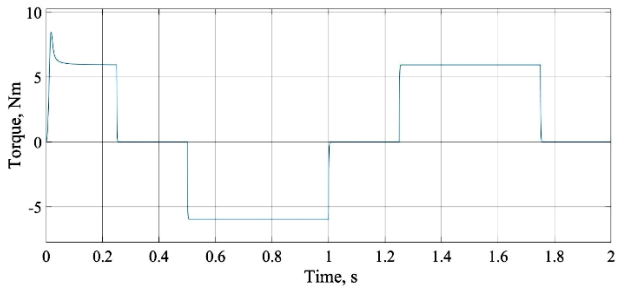

Fig. 21. Torque dependents in idle mode, Nm

Conclusions. Since the double-screw electromechanical hydrolyzer is a device that combines several technological processes, there is a need to maintain the exact parameters of the technological process. The simulation results were obtained under the following conditions: simulation time from 0 to 2 s with a step 0.5 s; the fixed value of the angular velocity at the torque step change is equal to the rated value; the time array of torque change is [0, 0.5, 0.75, 1, 1.25, 1.5] s; the time array of angular velocity cyclic change is [0, 0.25, 0.5, 1, 1.25, 1.7] s.

From the simulation results, the expediency of using the method of indirect control with field orientation in a double-screw electromechanical hydrolyzer is noticeable.

Compared to the considered control methods, indirect control with field orientation is simpler in design and implementation, allows to achieve the desired characteristics and opens further opportunities for the study of double-screw electromechanical hydrolyzer.

Conflict of interest. The authors of the paper state that there is no conflict of interest.

REFERENCES

1. Zablodskiy N., Kovalchuk S., Chuenko R., Romanenko O., Gritsyuk V. The nanofluids application in a twin-screw electromechanical hydrolyser. *2021 IEEE 21st International Conference on Nanotechnology (NANO)*, 2021, pp. 108-111. doi: https://doi.org/10.1109/NANO51122.2021.9514326.

2. Zablodskiy M., Kovalchuk S. The main aspects of the technology of processing keratin raw materials under the influence of a magnetic field. *2020 IEEE KhPI Week on Advanced Technology (KhPIWeek)*, 2020, pp. 278-282. doi: https://doi.org/10.1109/KhPIWeek51551.2020.9250153.

3. Yang S., Ding D., Li X., Xie Z., Zhang X., Chang L. A Novel Online Parameter Estimation Method for Indirect Field Oriented Induction Motor Drives. *IEEE Transactions on Energy Conversion*, 2017, vol. 32, no. 4, pp. 1562-1573. doi: https://doi.org/10.1109/TEC.2017.2699681.

4. Yan N., Cao X., Deng Z. Direct Torque Control for Switched Reluctance Motor to Obtain High Torque–Ampere Ratio. *IEEE Transactions on Industrial Electronics*, 2019, vol. 66, no. 7, pp. 5144-5152. doi: https://doi.org/10.1109/TIE.2018.2870355.

5. Kumar R.H., Iqbal A., Lenin N.C. Review of recent advancements of direct torque control in induction motor drives – a decade of progress. *IET Power Electronics*, 2018, vol. 11, no. 1, pp. 1-15. doi: https://doi.org/10.1049/iet-pel.2017.0252.

6. Wang F., Zhang Z., Mei X., Rodríguez J., Kennel R. Advanced Control Strategies of Induction Machine: Field Oriented Control, Direct Torque Control and Model Predictive Control. *Energies*, 2018, vol. 11, no. 1. doi: https://doi.org/10.3390/en11010120.

7. Amezquita-Brooks L., Liceaga-Castro J., Liceaga-Castro E. Speed and Position Controllers Using Indirect Field-Oriented Control: A Classical Control Approach. *IEEE Transactions on Industrial Electronics*, 2014, vol. 61, no. 4, pp. 1928-1943. doi: https://doi.org/10.1109/TIE.2013.2262750.

8. De Oliveira V M.R., Camargo R.S., Encarnação L.F. Field Oriented Predictive Current Control on NPC Driving an Induction Motor. *2020 IEEE International Conference on Industrial Technology (ICIT)*, 2020, pp. 169-174. doi: https://doi.org/10.1109/ICIT45562.2020.9067236.

9. Benbouhenni H. Seven-Level Direct Torque Control of Induction Motor Based on Artificial Neural Networks with Regulation Speed Using Fuzzy PI Controller. *Iranian Journal of Electrical and Electronic Engineering*, 2018, vol. 14, no. 1, pp. 85-94. doi: http://dx.doi.org/10.22068/IJEEE.14.1.85.

10. Nikzad M.R., Asaei B., Ahmadi S.O. Discrete Duty-Cycle-Control Method for Direct Torque Control of Induction Motor Drives With Model Predictive Solution. *IEEE Transactions on Power Electronics*, 2018, vol. 33, no. 3, pp. 2317-2329. doi: https://doi.org/10.1109/TPEL.2017.2690304.

11. Mousavi M.S., Davari S.A., Nekoukar V., Garcia C., Rodriguez J. A Robust Torque and Flux Prediction Model by a Modified Disturbance Rejection Method for Finite-Set Model-Predictive Control of Induction Motor. *IEEE Transactions on Power Electronics*, 2021, vol. 36, no. 8, pp. 9322-9333. doi: https://doi.org/10.1109/TPEL.2021.3054242.

12. Ekaputri C., Syaichu-Rohman A. Model predictive control (MPC) design and implementation using algorithm-3 on board SPARTAN 6 FPGA SP605 evaluation kit. *2013 3rd International Conference on Instrumentation Control and Automation (ICA)*, 2013, pp. 115-120. doi: https://doi.org/10.1109/ICA.2013.6734056.

13. Wang L. *Model Predictive Control System Design and Implementation Using MATLAB®*. Springer, London, 2009. doi: https://doi.org/10.1007/978-1-84882-331-0.

14. Zablodsky N., Chuenko R., Gritsyuk V., Kovalchuk S., Romanenko O. The Numerical Analysis of Electromechanical Characteristics of Twin-Screw Electromechanical Hydrolyzer. *2021 11th International Conference on Advanced Computer Information Technologies (ACIT)*, 2021, pp. 130-135. doi: https://doi.org/10.1109/ACIT52158.2021.9548392.

15. Zablodskiy M., Pliuhin V., Chuenko R. Simulation of induction machines with common solid rotor. *Technical Electrodynamics*, 2018, no. 6, pp. 42-45. doi: https://doi.org/10.15407/techned2018.06.042.

16. Hiware R.S., Chaudhari J.G. Indirect Field Oriented Control for Induction Motor. *2011 Fourth International Conference on Emerging Trends in Engineering & Technology*, 2011, pp. 191-194. doi: https://doi.org/10.1109/ICETET.2011.56.

17. Abu-Rub H., Iqbal A., Guziński J. *High Performance Control of AC Drives with MATLAB/Simulink Models*. John Wiley & Sons, 2012. doi: https://doi.org/10.1002/9781119969242.

18. Malyar V.S., Hamola O.Ye., Maday V.S., Vasylchyshyn I.I. Mathematical modelling of starting modes of induction motors with squirrel-cage rotor. *Electrical Engineering & Electromechanics*, 2021, no. 2, pp. 9-15. doi: https://doi.org/10.20998/2074-272X.2021.2.02.

19. Shurub Yu.V. Statistical optimization of frequency regulated induction electric drives with scalar control. *Electrical engineering & electromechanics*, 2017, no. 1, pp. 26-30. doi: https://doi.org/10.20998/2074-272X.2017.1.05.

Received 24.11.2021
Accepted 26.12.2021
Published 23.02.2022

M.M. Zablodskiy[1], *Doctor of Technical Science, Professor,*
V.E. Pliuhin[2], *Doctor of Technical Science, Professor,*
S.I. Kovalchuk[1], *Postgraduate Student,*
V.O. Tietieriev[2], *Postgraduate Student,*
[1] National University of Life and Environmental Sciences of Ukraine, 12, Heroyiv Oborony Str., Kyiv, 03041, Ukraine,
e-mail: zablodskiynn@gmail.com, kovalchuk@it.nubip.edu.ua
[2] O.M. Beketov National University of Urban Economy on Kharkiv, 17, Marshal Bazhanov Str., Kharkiv, 61002, Ukraine,
e-mail: vladyslav.pliuhin@kname.edu.ua (Corresponding author), vitaliy.teterev@kname.edu.ua

How to cite this article:
Zablodskiy M.M., Pliuhin V.E., Kovalchuk S.I., Tietieriev V.O. Indirect field-oriented control of twin-screw electromechanical hydrolyzer. *Electrical Engineering & Electromechanics*, 2022, no. 1, pp. 3-11. doi: https://doi.org/10.20998/2074-272X.2022.1.01.